



# Production of middle distillate in a dual-bed reactor from synthesis gas through wax cracking: Effect of acid property of Pd-loaded solid acid catalysts on the wax conversion and middle distillate selectivity

Kyung Min Cho<sup>a</sup>, Sunyoung Park<sup>a</sup>, Jeong Gil Seo<sup>a</sup>, Min Hye Youn<sup>a</sup>, Sung-Hyeon Baek<sup>b</sup>, Ki-Won Jun<sup>c</sup>, Jin Suk Chung<sup>d</sup>, In Kyu Song<sup>a,\*</sup>

<sup>a</sup> School of Chemical and Biological Engineering, Institute of Chemical Processes, Seoul National University, Shinlim-dong, Kwanak-ku, Seoul 151-744, South Korea

<sup>b</sup> Department of Chemical Engineering, Inha University, Incheon 402-751, South Korea

<sup>c</sup> Korea Research Institute of Chemical Technology, Daejeon 305-600, South Korea

<sup>d</sup> School of Chemical Engineering and Bioengineering, University of Ulsan, Ulsan 680-749, South Korea

## ARTICLE INFO

### Article history:

Received 28 December 2007

Received in revised form 22 February 2008

Accepted 24 February 2008

Available online 29 February 2008

### Keywords:

Fischer–Tropsch synthesis (FTS)

Synthesis gas

Middle distillate

Dual-bed reactor

Wax cracking

## ABSTRACT

Selective production of middle distillate (C<sub>10</sub>–C<sub>20</sub>) from synthesis gas (CO + H<sub>2</sub>) was carried out in a dual-bed reactor. Co-based catalysts were used in the first-bed reactor to produce wax (C<sub>21+</sub>) from synthesis gas, and Pd-loaded solid acid catalysts were used in the second-bed reactor to produce middle distillate from wax through hydrocracking. Co/TiO<sub>2</sub> catalyst in the first-bed reactor produced more than 35 wt% middle distillate and more than 20 wt% wax. These products served as a suitable feed for the production of middle distillate through hydrocracking in the second-bed reactor. Pd-loaded solid acid catalysts used in the second-bed reactor retained three types of acid sites (weak-, medium-, and strong-acid sites). Correlations between medium acidity and catalytic activity of Pd-loaded solid acid catalyst revealed that wax conversion and increment of middle distillate selectivity in the second-bed reactor were increased with increasing medium acidity of the catalyst. Total acidity of Pd-loaded solid acid catalyst was increased with increasing medium acidity of the catalyst. Thus, the medium acidity (total acidity) of Pd-loaded solid acid catalyst served as a crucial factor in hydrocracking of wax. Among the second-bed catalysts, the Pd/mesoporous alumina (Pd/MA) catalyst with the highest medium acidity (total acidity) showed the best catalytic performance (ca. 83% wax conversion and ca. 15 wt% increment of middle distillate selectivity).

© 2008 Elsevier B.V. All rights reserved.

## 1. Introduction

Fischer–Tropsch synthesis (FTS) is a well-known process for producing high-quality fuels and petrochemicals from synthesis gas (CO + H<sub>2</sub>) which can be easily obtained from other organic resources such as coal, biomass, and natural gas [1–3]. FTS has been spotlighted as one of the major gas conversion routes for gas-to-liquid (GTL), coal-to-liquid (CTL), and biomass-to-liquid (BTL) processes [2,3]. FTS has also attracted much attention as a promising process for producing clean fuels as a result of the implementation of more stringent environmental legislations on fuel oil [1,4,5]. It is expected within the next decades that both gasoline and diesel fuels will be restricted to have ultra-low sulfur concentration, while the hydrocarbon fuel spectrum will shift from

aromatics and olefins to naphthenes and *iso*-paraffins [6]. Diesel fuel obtained from FTS retains extremely low sulfur and aromatic contents, high-cetane index, and clean burning feature in compression-ignition engines [7]. Furthermore, FTS diesel fuel shows low emission of CO, nitrogen oxides, hydrocarbons, and other particulates.

FTS with conventional supported metal catalysts yields a wide spectrum of hydrocarbons, because the product distribution is controlled by the Anderson–Schulz–Flory (ASF) polymerization kinetics [1,2,8–11]. This imposes a limitation on the maximum selectivity for a given hydrocarbon product. It is known that the theoretical maximum selectivity for gasoline (C<sub>5</sub>–C<sub>11</sub>) is ca. 48%, while that for middle distillate (C<sub>10</sub>–C<sub>20</sub>) is ca. 40% [8,12]. In order to overcome the limitation of ASF distribution in the FTS, several hybrid FTS catalyst systems have been developed [9,13–16]. The hybrid FTS catalyst is composed of a typical Fischer–Tropsch (FT) catalyst and an acid catalyst. The function of acid catalyst in the hybrid catalyst is to convert long-chain paraffins

\* Corresponding author. Tel.: +82 2 880 9227; fax: +82 2 888 7295.

E-mail address: [inksong@snu.ac.kr](mailto:inksong@snu.ac.kr) (I.K. Song).

(FT product) into the desired products through cracking [9,13]. A number of zeolites have been employed as an acid catalyst for the hybrid FTS catalyst system with an aim of producing gasoline. It has been reported that a combination of ZSM-5 with a FT catalyst promoted the production of aromatics and branched paraffins by secondary reactions of the primary products formed by FT catalyst. For example, gasoline selectivity more than 70% was obtained using KFeCo catalyst supported on ZSM-5 [8]. Botes [17] investigating a Fe-based FT catalyst combined with ZSM-5 reported that the acidity of ZSM-5 strongly affected the catalytic activity and product selectivity. Another work also revealed that a hybrid catalyst composed of a physical mixture of Co-based catalyst and zeolite enhanced the selectivity for middle *iso*-paraffins [18].

In the production of heavy hydrocarbons such as diesel ( $C_{12}$ – $C_{18}$ ) or middle distillate ( $C_{10}$ – $C_{20}$ ), the main problem of single-bed hybrid FTS system is the difference in optimal operating conditions between FTS reaction and hydrocarbon conversion reaction. Solid acids for the hydrocracking and hydroisomerization of FTS products are highly active at reaction temperature higher than 280 °C [19]. At this temperature, however, long-chain hydrocarbons cannot be produced, because the polymerization over FT catalyst is not favorable at high temperature [20,21]. On the other hand, long-chain hydrocarbons are favorably produced at 220 °C over FT catalyst, but the hydrocracking and hydroisomerization hardly occur over solid acid catalysts at 220 °C. Furthermore, the acid site of single-bed hybrid FTS catalyst system plays a role in suppressing the formation of long-chain hydrocarbons. All these imply that both FTS and hydrocracking cannot be efficiently conducted in a single-bed reactor for production of heavy hydrocarbons such as middle distillate.

In order to overcome this problem, a dual-bed reactor system has been employed in the hybrid FTS system [14,15]. It has been reported that a combination of Co-based FT catalyst with metal/zeolite catalyst in a dual-bed reactor system enhanced the production of gasoline-range *iso*-paraffins [1,7,10,22]. The dual-bed reactor system is consisted of two serial reactors; the first-bed reactor contains a FT catalyst for FTS and the second-bed reactor contains a hydrocracking catalyst. The advantage of dual-bed reactor system is that each reactor can be operated independently under the optimal operating conditions to obtain a desired product [19]. Up to the present, most of the hybrid FTS catalytic reactors have been developed for the production of gasoline [10,11,18,19,22,23]. Although much progress has not been made on the hybrid FTS system for the production of middle distillate, it has been reported that high yield for middle distillate can be obtained by a two-step process; a low-temperature FTS over Co-based catalyst for the production of long-chain *n*-paraffin (wax) in the first-bed reactor, and a subsequent hydrocracking of wax into middle distillate in the second-bed reactor [24].

In this work, selective production of middle distillate in a dual-bed reactor from synthesis gas through wax cracking was conducted. Co-based catalysts were chosen as an efficient FTS catalyst for the production of wax from synthesis gas in the first-bed reactor. In the second reactor, a number of Pd-loaded solid acid catalysts were examined for the production of middle distillate from wax through hydrocracking. It is known that the hydrocracking is generally carried out over a metal/acid bifunctional catalyst. Alkanes are dehydrogenated on the metallic sites and then isomerized or cracked on the acid sites through classical or non-classical carbenium ion chemistry [25–28]. The effect of acid property of Pd-loaded solid acid catalysts on the wax conversion and middle distillate selectivity was extensively investigated.

## 2. Experimental

### 2.1. Preparation of first-bed catalyst

Co-based catalysts for FTS were prepared by an incipient wetness impregnation method for use in the first-bed reactor. Cobalt nitrate ( $\text{Co}(\text{NO}_3)_2 \cdot 6\text{H}_2\text{O}$ , Sigma–Aldrich) was used as a cobalt precursor.  $\text{TiO}_2$  (P25, Degussa), mesoporous silica (SBA-15), and  $\text{SiO}_2$  (R972, Degussa) were used as a support. A mesoporous silica (SBA-15) was prepared according to the reported method [29]. The loading of Co on  $\text{TiO}_2$ , SBA-15, and  $\text{SiO}_2$  was fixed at 15 wt%. Co/ $\text{SiO}_2$  and Co/SBA-15 catalysts were calcined at 500 °C for 5 h, while Co/ $\text{TiO}_2$  catalyst was calcined at 300 °C for 20 h [30].

### 2.2. Preparation of second-bed catalyst

Five aluminas and one silica materials were used as an acid support for Pd catalyst. A mesoporous alumina (MA) was prepared according to the method reported in the literature [31], and it was calcined at 500 °C for 5 h. Xerogel aluminas were also synthesized according to the reported method [32]. The xerogel aluminas were separately calcined at 900 and 1000 °C for 5 h (denoted as XA900 and XA1000, respectively). Acidic alumina (Sigma–Aldrich, denoted as AA) and commercial alumina (Degussa, denoted as DA) were used as-received. A mesoporous silica (SBA-15, denoted as MS) was prepared according to the reported method [29], and it was calcined at 500 °C for 5 h.

All the Pd-loaded solid acid catalysts were prepared by an impregnation method using a known amount of palladium precursor ( $\text{Pd}(\text{NO}_3)_2$ , Sigma–Aldrich). The loading of Pd on each acid support was fixed at 1 wt%. After drying the impregnated catalysts overnight at 100 °C, they were calcined at 500 °C for 5 h. The prepared catalysts were denoted as Pd/MA, Pd/XA900, Pd/XA1000, Pd/AA, Pd/DA, and Pd/MS.

### 2.3. Catalyst characterization

Acid properties of Pd-loaded solid acid catalysts were measured by  $\text{NH}_3$ -TPD experiments. Each catalyst (0.2 g) was charged into a tubular quartz reactor of the conventional TPD apparatus. The catalyst was pretreated at 400 °C for 3 h under a flow of hydrogen (5 ml/min) and helium (10 ml/min) to reduce the catalyst. 20 ml of  $\text{NH}_3$  was then pulsed into the reactor every minute at room temperature under a flow of helium (5 ml/min), until the acid sites were saturated with  $\text{NH}_3$ . The physisorbed  $\text{NH}_3$  was removed by evacuating the catalyst sample at 50 °C for 1 h. The furnace temperature was increased from room temperature to 1000 °C at a heating rate of 5 °C/min under a flow of helium (10 ml/min). The desorbed  $\text{NH}_3$  was detected using a GC (Younglin, ACME 6000, TCD).

### 2.4. Catalytic reaction

The reaction was carried out in a dual-bed fixed-bed reactor. The scheme for the dual-bed reactor system is presented in Fig. 1. Both first-bed and second-bed reactors (SUS, ID = 8 mm) were consecutively arranged in the vertical direction. In the first-bed reactor, a FT catalyst (Co/ $\text{TiO}_2$ , Co/SBA-15 or Co/ $\text{SiO}_2$ ) was loaded to produce long-chain hydrocarbons. In the second-bed reactor, a Pd-loaded solid acid catalyst was loaded for hydrocracking of wax from the first-bed reactor. 0.3 g of FT catalyst (Co/ $\text{TiO}_2$ , Co/SBA-15 or Co/ $\text{SiO}_2$ ) diluted with 0.5 g of quartz sand was charged in the first-bed reactor. The FTS reaction in the first-bed reactor was conducted under the conditions of  $P = 10$  bar,  $\text{H}_2/\text{CO} = 2.0$ ,  $W/F = 20.0$  g-cat-h/mol, and  $T = 220$  °C. 0.3 g of Pd-loaded solid acid catalyst was used in the second-bed reactor. Additional  $\text{H}_2$  was

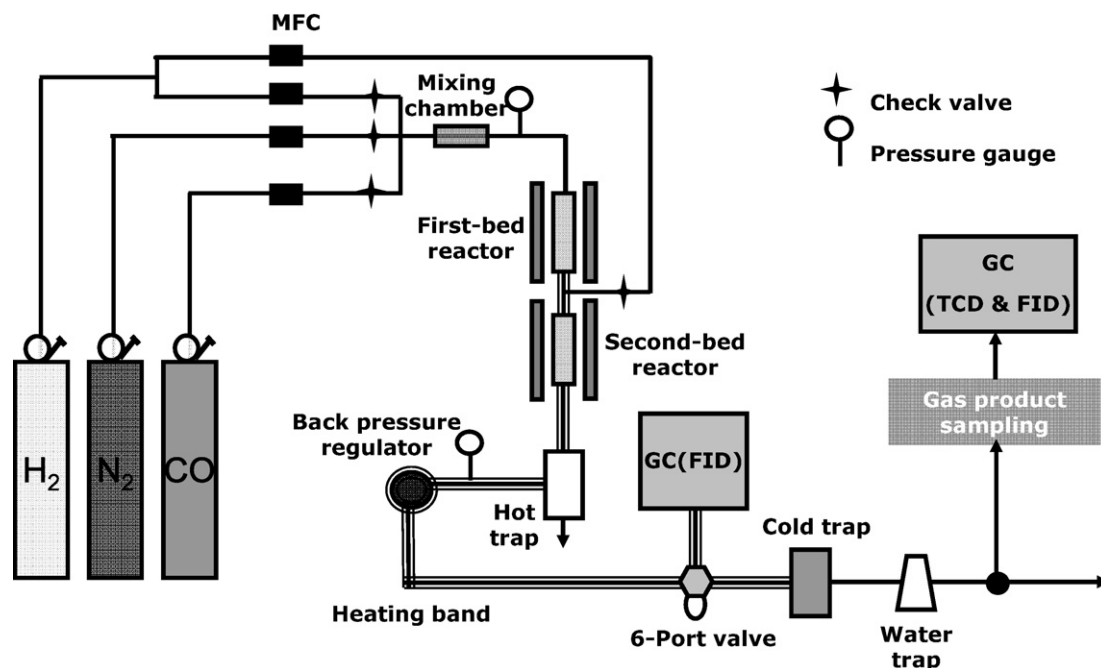


Fig. 1. Scheme for the dual-bed reactor system.

introduced into the second-bed reactor, where  $H_2/CO$  ratio was fixed at 2.5 by assuming no reaction in the first-bed reactor. The reaction in the second-bed reactor was conducted under the condition of  $P = 10$  bar and  $T = 330$  °C. Prior to the reaction, Co/SBA-15 and Co/SiO<sub>2</sub> were reduced at 400 °C for 16 h, and Co/TiO<sub>2</sub> was reduced at 250 °C for 16 h. Pd-loaded solid acid catalysts in the second-bed reactor were reduced at 400 °C for 16 h. All the reaction experiments were conducted more than 7 h under the steady-state condition.

Effluent hydrocarbon products which were not condensed at a hot trap were analyzed using an on-line GC (HP 5890II, Agilent) equipped with a FID. CO, CH<sub>4</sub>, and CO<sub>2</sub> in the effluent system from a water trap were analyzed using a GC (Younglin, 600 D) equipped with a TCD, and light hydrocarbons (C<sub>1</sub>–C<sub>5</sub>) in the effluent stream were also analyzed using a GC (Younglin, 600 D) equipped with a FID. Heavy hydrocarbon products (C<sub>10+</sub>) collected from a hot trap were analyzed using a GC (HP 5890II, Agilent) equipped with a FID. The reaction data in each reactor were obtained after a 7-h reaction. For more accurate analysis, the liquid product was collected for 7 h without samplings. CO conversion and hydrocarbon selectivity were calculated according to the following equations:

$$\text{CO conversion (\%)} = \frac{(\text{weight of CO introduced}) - (\text{weight of CO unreacted})}{(\text{weight of CO introduced})} \quad (1)$$

$$\text{Hydrocarbon selectivity (wt\%)} = \frac{(\text{weight of specific hydrocarbon produced})}{(\text{weight of total hydrocarbon produced})} \quad (2)$$

### 3. Results and discussion

#### 3.1. FTS reaction in the first-bed reactor

It is desired to produce heavy hydrocarbons (middle distillate and wax) through FTS in the first-bed reactor. In this work, therefore, we attempted to find an efficient catalyst showing high selectivity for middle distillate and wax. Co-based catalyst is known to be a

promising catalyst for the production of long-chain paraffins in low-temperature FTS [33–35]. To find a suitable catalyst for the first-bed reactor, Co/SiO<sub>2</sub>, Co/SBA-15, and Co/TiO<sub>2</sub> were examined. CO conversion, hydrocarbon selectivity, and chain growth probability ( $\alpha$ ) over these three catalysts, which were obtained under the condition of blank second-bed reactor, are summarized in Table 1. As listed in Table 1, Co/SiO<sub>2</sub> catalyst showed high selectivity for methane and low selectivity for liquid product. Co/SBA-15 catalyst also showed low selectivity for liquid product. This means that Co/SiO<sub>2</sub> and Co/SBA-15 are not suitable to provide sufficient amounts of middle distillate and wax products to the second-bed reactor, where hydrocracking occurs to produce middle distillate. On the other hand, Co/TiO<sub>2</sub> catalyst showed low selectivity for methane. Furthermore, Co/TiO<sub>2</sub> catalyst exhibited high selectivity for middle distillate and wax enough to be used as a feed for the second-bed reactor. These results are in good agreement with the previous reports [30,36–40]. Based on these results, Co/TiO<sub>2</sub> was chosen as a suitable catalyst for the first-bed reactor.

Fig. 2 shows the carbon number distribution over Co/TiO<sub>2</sub> catalyst in the first-bed reactor. It shows a typical ASF distribution, and the maximum selectivity (except for methane) was observed at the carbon number of 15. This means that theoretical maximum selectivity for middle distillate was obtained and sufficient amount of wax was produced in the first-bed reactor. The amount of wax produced in the first-bed reactor is very important in increasing selectivity for middle distillate through hydrocracking in the second-bed reactor. Chain growth probability ( $\alpha$ ) over Co/TiO<sub>2</sub> catalyst in the first-bed reactor is shown in Fig. 3. The chain growth probability ( $\alpha$ ) value over Co/TiO<sub>2</sub> catalyst was in the range of

**Table 1**  
Catalytic activity of Co/SiO<sub>2</sub>, Co/SBA-15, and Co/TiO<sub>2</sub> for FTS in the first-bed reactor

Catalyst	CO conversion (%)	Hydrocarbon selectivity (wt%)				Chain growth probability ( $\alpha$ )
		C <sub>1</sub>	C <sub>10</sub> –C <sub>20</sub>	C <sub>21</sub> +	C <sub>5</sub> +	
Co/SiO <sub>2</sub>	56.7	22.7	23.5	2.5	59.8	0.74
Co/SBA-15	67.7	10.1	26.3	1.0	73.4	0.78
Co/TiO <sub>2</sub>	69.2	8.9	37.0	23.9	84.6	0.89

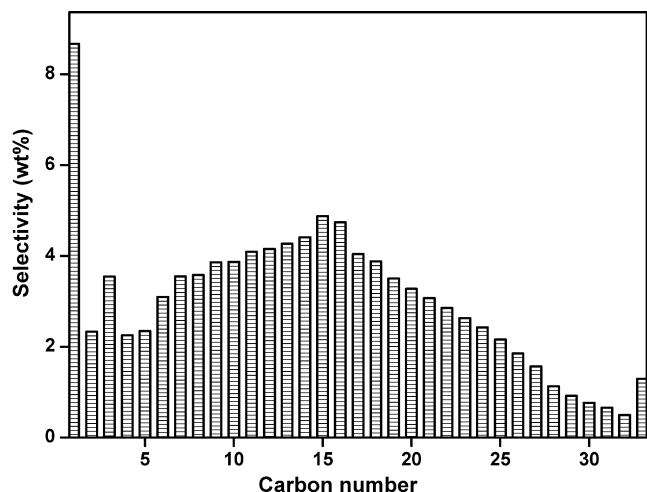


Fig. 2. Carbon number distribution over Co/TiO<sub>2</sub> catalyst in the first-bed reactor ( $T = 220\text{ }^{\circ}\text{C}$ ,  $P = 10\text{ bar}$ ,  $\text{H}_2/\text{CO} = 2$ , reaction time = 7 h).

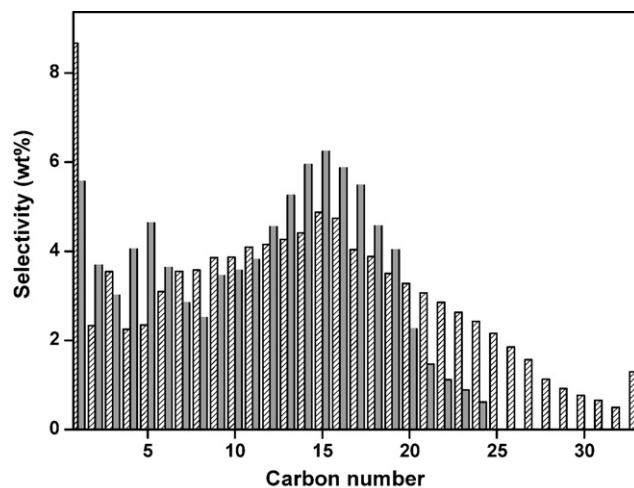


Fig. 4. Typical carbon number distributions in the first-bed reactor and in the dual-bed reactor: (▨) Co/TiO<sub>2</sub> (first-bed only); (■) Co/TiO<sub>2</sub> (first-bed) + Pd/MA (second-bed).

0.88–0.94. It is noticeable that the chain growth probability over Co/TiO<sub>2</sub> catalyst slightly decreased at around the carbon number of 16, although it is known that the  $\alpha$  value increases with increasing carbon number [41,42]. In fact, the FT product spectrum is very difficult to analyze quantitatively, because a very wide carbon number distribution is covered and normally different product fractions are analyzed individually and then added together to obtain the full product spectrum. Although the abnormal behavior of ASF distribution might be due to a certain analytical error, many efforts were made to minimize analytical errors and to get reproducible data in this work. Therefore, it is believed that the possibility of analytical errors is very low. The abnormal behavior can be explained by the fact that the chain growth probability over Co-based FT catalyst changes with increasing reaction time and the data shown in Fig. 2 represent the carbon number distribution of accumulated product for 7 h. The collected sample includes the products of unsteady-state reaction at the initial stage. Thus, the ASF spectrum over Co/TiO<sub>2</sub> catalyst showed a slightly different behavior from that in the literatures [43–45]. Nonetheless, it was revealed that more than 35 wt% middle distillate and more than 20 wt% wax were continuously produced in the first-bed reactor. These products could be utilized as a suitable feed for the production of middle distillate through hydrocracking in the second-bed reactor.

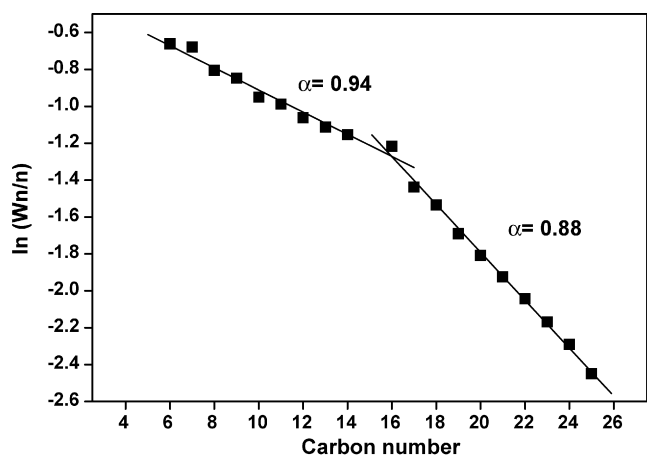


Fig. 3. Chain growth probability ( $\alpha$ ) over Co/TiO<sub>2</sub> catalyst in the first-bed reactor ( $T = 220\text{ }^{\circ}\text{C}$ ,  $P = 10\text{ bar}$ ,  $\text{H}_2/\text{CO} = 2$ , reaction time = 7 h).

### 3.2. Wax cracking in the second-bed reactor

Fig. 4 shows the typical carbon number distributions in the first-bed reactor (Co/TiO<sub>2</sub>) and in the dual-bed reactor (Co/TiO<sub>2</sub> + Pd/MA). Fig. 4 clearly shows that wax produced in the first-bed reactor was mainly cracked to middle distillate. The selectivity for middle distillate in the dual-bed reactor was ca. 15 wt% higher than that in the first-bed reactor. The selectivity for light hydrocarbons (C<sub>2</sub>–C<sub>4</sub>) in the dual-bed reactor was also slightly increased compared to that in the first-bed reactor. The above results were due to the hydrocracking of heavy hydrocarbons in the second-bed reactor. It should be emphasized that the selective cracking of wax to middle distillate is desirable without the cracking of hydrocarbons with the carbon number lower than 20. It is also noteworthy that the selectivity increment of gasoline-range hydrocarbon and light hydrocarbon was not significant compared to that of middle distillate. Such a product distribution may be explained by the reaction mechanism referred to as pure primary cracking; C–C bond scission on centrally situated carbon atom is favored. This mechanism contributes to the strong dependence of paraffin reactivity on chain length. It has been reported that the intrinsic cracking activity of *n*-paraffins increases with increasing carbon chain length [1,3,12,24]. It has also been reported that long chain hydrocarbons have a high propensity to be adsorbed onto the catalyst. Because the degree of adsorption on the catalyst surface exponentially increases in hydrocarbons with carbon number more than 20 [24], the selective hydrocracking of heavy hydrocarbons can occur. It can be said all these led to the increment of middle distillate selectivity by the selective hydrocracking of wax over the Pd-loaded solid acid catalyst.

Carbon number distributions over various Pd-loaded solid acid catalysts are summarized in Table 2. Although no great difference in methane selectivity between dual-bed reactor (Table 2) and first-bed reactor (Table 1) was observed, the selectivity for methane in the dual-bed reactor was slightly lower than that in the first-bed reactor in some cases. It has been reported that the characteristic feature of Pd-containing hybrid catalyst system is responsible for such a low-methane selectivity [1,10,18]. It is known that methane can be formed from not only FTS itself but also from olefins.  $\alpha$ -Olefins can be cracked to produce methane. Therefore, one may expect that methane selectivity in the dual-bed reactor system would be slightly higher than that formed by FTS. When a Pd-loaded solid acid catalyst was employed in the second-bed reactor, however,  $\alpha$ -olefins were effectively hydrogenated.



**Table 2**

Carbon number distributions over Pd-loaded solid acid catalysts in the second-bed reactor

Catalyst	Hydrocarbon selectivity (wt%)				
	C <sub>1</sub>	C <sub>2</sub> –C <sub>4</sub>	C <sub>10</sub> –C <sub>20</sub>	C <sub>21</sub> +	C <sub>5</sub> +
Pd/MA	5.6	13.7	51.6	4.1	80.7
Pd/XA900	7.5	12.7	46.9	11.5	79.8
Pd/AA	9.3	9.2	44.9	10.8	81.5
Pd/DA	5.0	12.3	42.8	13.8	82.7
Pd/XA1000	5.7	10.5	44.9	17.2	83.8
Pd/MS	6.0	4.3	43.4	20.2	89.7

Thus, the formation of methane derived from the secondary cracking reaction of  $\alpha$ -olefin disappeared [18]. As an evidence for olefin hydrogenation, it was revealed that the dual-bed reaction with a Pd-containing catalyst showed a lower selectivity for  $\alpha$ -olefin than the FTS reaction alone. The olefin/paraffin ratios in C<sub>2</sub>–C<sub>4</sub> hydrocarbons decreased when a Pd-loaded solid acid catalyst was employed in the second-bed reactor (olefin/paraffin ratios in C<sub>2</sub>–C<sub>4</sub> hydrocarbons: first-bed = 0.36, Pd/MA = 0.14, Pd/XA900 = 0.16, Pd/AA = 0.31, Pd/DA = 0.16, Pd/XA1000 = 0.13, Pd/MS = 0.15).

Table 3 shows the wax conversion and increment of middle distillate selectivity in the second-bed (dual-bed) reactor, which were calculated according to the following equations. It is noticeable that the selectivity for middle distillate in the dual-bed reactor remarkably increased (5.8–14.6 wt%) compared to that in the first-bed reactor, which was attained by the selective hydrocracking of wax:

Wax conversion (%)

$$= \frac{23.9 \text{ wt\% (wt\% of wax formed in the first-bed reactor)} - (\text{wt\% of wax remained in the second-bed reactor})}{23.9 \text{ wt\% (wt\% of wax formed in first-bed reactor)}} \quad (3)$$

Increment of middle distillate selectivity (wt%)

$$= (\text{wt\% of middle distillate in the second-bed reactor}) - 37.0 \text{ wt\% (wt\% of middle distillate formed in the first-bed reactor)} \quad (4)$$

Fig. 5 shows the correlation between wax conversion and increment of middle distillate selectivity in the second-bed reactor. It is interesting to note that the increment of middle distillate selectivity was not directly proportional to the wax conversion, but was roughly increased with increasing wax conversion. This implies that the increment of middle distillate selectivity was mainly due to the wax cracking. The increment of middle distillate selectivity was attributed to the second-bed catalysis. This implies that the formation of middle distillate by hydrocracking reaction would be different depending on the identity of second-bed catalyst.

**Table 3**

Wax conversion and increment of middle distillate selectivity in the second-bed reactor

Catalyst	Wax conversion (%)	Increment of middle distillate selectivity (wt%)
Pd/MA	82.8	14.6
Pd/XA900	51.9	9.9
Pd/AA	54.8	7.9
Pd/DA	42.3	5.8
Pd/XA1000	28.0	7.9
Pd/MS	15.5	6.4

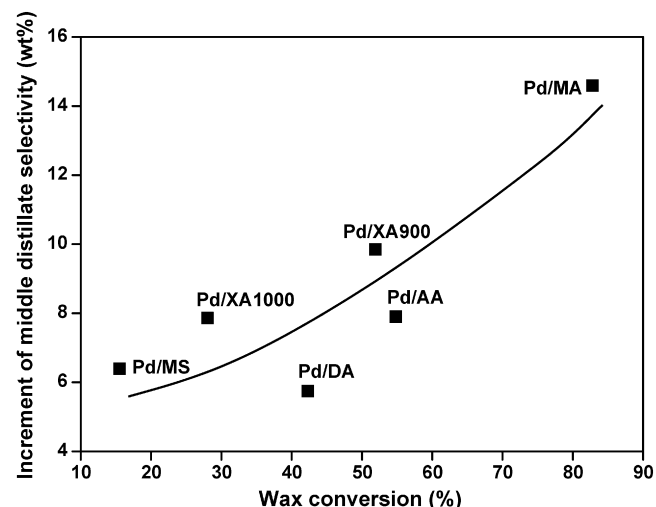


Fig. 5. A correlation between wax conversion and increment of middle distillate selectivity in the second-bed reactor.

### 3.3. Effect of acid property of Pd-loaded solid acid catalyst

In order to investigate the effect of acid properties of Pd-loaded solid acid catalysts on the wax conversion and middle distillate selectivity, NH<sub>3</sub>-TPD measurements were conducted. Fig. 6 shows the NH<sub>3</sub>-TPD profiles of selected Pd-loaded solid acid catalysts. As shown in Fig. 6, there are three types of acid sites in all catalysts. A low-temperature peak in the range of 170–200 °C, a medium-temperature peak in the range of 240–300 °C, and a high-temperature peak in the range of 580–650 °C correspond to weak-, medium-, and strong-acid sites, respectively. Medium-acid sites appeared as a shoulder in some cases. However, acidity of each acid site could be determined by deconvoluting the NH<sub>3</sub>-TPD profile. Acidities of Pd-loaded solid acid catalysts are summarized in Table 4. The result clearly shows that the supported Pd catalysts retained a wide spectrum of total acidity depending on the identity of solid acid support. Some attempts have been made to correlate the acid property with the hydrocracking activity of Pd-loaded solid acid catalyst. Fig. 7 shows the correlation between medium acidity and wax conversion in the second-bed reactor. The correlation clearly shows that wax conversion was increased with increasing medium acidity of second-bed catalyst. However, no

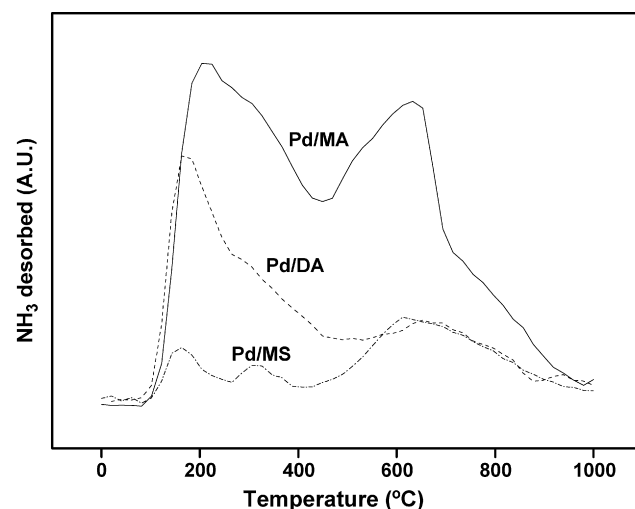


Fig. 6. NH<sub>3</sub>-TPD profiles of selected Pd-loaded solid acid catalysts.

**Table 4**  
Acidities of Pd-loaded solid acid catalysts

Catalyst	Acidity (mmol-NH <sub>3</sub> /g-catalyst)			
	Weak-acid site (170–200 °C)	Medium-acid site (240–300 °C)	Strong-acid site (580–650 °C)	Total acidity
Pd/MA	0.19	0.44	0.83	1.46
Pd/XA900	0.26	0.35	0.57	1.18
Pd/AA	0.10	0.33	0.53	0.96
Pd/DA	0.15	0.25	0.29	0.69
Pd/XA1000	0.14	0.13	0.29	0.56
Pd/MS	0.04	0.02	0.29	0.35

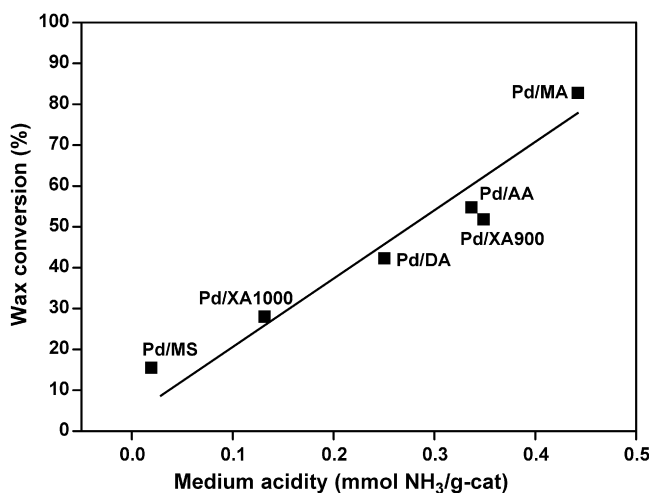
reliable correlation between wax conversion and weak/strong acidity was observed. The correlation between medium acidity and cracking activity shown in Fig. 7 is well consistent with the previous reports [25,46–50]. It has been reported that the rate constant for each step in the catalytic cracking reaction was proportional to the medium acidity of the catalyst. Furthermore, it is known that the reaction rate is accelerated by the medium-acid sites in the monomolecular reaction (the cracking of carbonium ion formed by protonation of feed molecule) [50–52]. This supports

that the medium acidity served as a crucial factor in hydrocracking of wax.

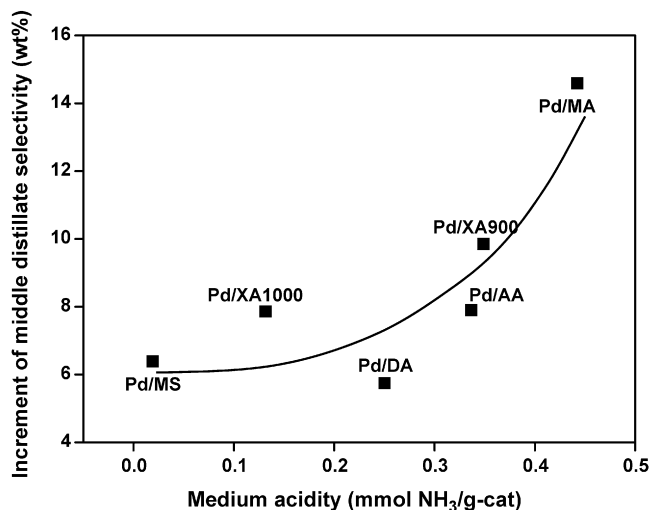
Although the increment of middle distillate selectivity was not directly proportional to the wax conversion (Table 3 and Fig. 5), a reliable correlation between medium acidity and increment of middle distillate selectivity could be established (Fig. 8). As shown in Fig. 8, the increment of middle distillate selectivity in the second-bed reactor was roughly increased with increasing medium acidity of Pd-loaded solid acid catalyst. Once again, this result supports that the medium acidity of Pd-loaded solid acid catalyst played an important role in hydrocracking of wax to middle distillate. Among the second-bed catalysts, the Pd/MA catalyst with the highest medium acidity showed the best catalytic performance (Figs. 7 and 8). The Pd/MA catalysts exhibited ca. 83% wax conversion and ca. 15 wt% increment of middle distillate selectivity, when compared to the effluent stream from the first-bed reactor (Table 3).

Fig. 9 shows the correlation between total acidity and medium acidity of Pd-loaded solid acid catalysts established from data in Table 4. It is interesting to note that total acidity of Pd-loaded solid acid catalyst was increased with increasing medium acidity of the catalyst. Therefore, the dependencies of wax conversion and increment of middle distillate selectivity on total acidity showed the same trends as those shown in Figs. 7 and 8. In this work, wax conversion and increment of middle distillate selectivity were increased with increasing total acidity of Pd-loaded solid acid catalyst. However, the effect of total acidity on the cracking ability of the catalyst is still debatable [50,53].

Water (steam) is produced from FT reaction. Co-based catalyst has low activity for water gas shift reaction, and therefore, water (steam) may be presented in the reaction system. This means that



**Fig. 7.** A correlation between medium acidity and wax conversion in the second-bed reactor.



**Fig. 8.** A correlation between medium acidity and increment of middle distillate selectivity in the second-bed reactor.

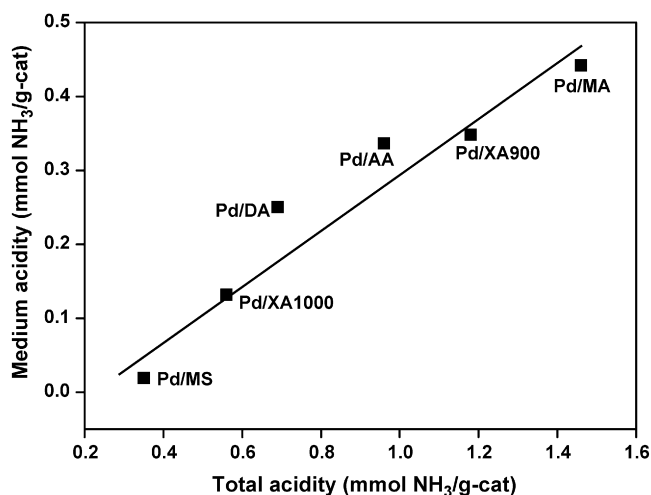


**Fig. 9.** A correlation between total acidity and medium acidity of Pd-loaded solid acid catalysts.

water (steam) contacts the solid acid catalyst directly. However, it was reported that neither interaction of water with the OH groups nor formation of new hydroxyl groups was observed at the cracking reaction [54]. In other words, water (steam) plays a role of inert stream, improving the dispersion of hydrocarbon feed. Thus, the effect of water (steam) on the acid site of solid acid catalyst is negligible.

#### 4. Conclusions

Selective production of middle distillate in a dual-bed reactor from synthesis gas through wax cracking was conducted. Co-based catalysts were used in the first-bed reactor to produce wax from synthesis gas, and Pd-loaded solid acid catalysts were used in the second-bed reactor for the production of middle distillate from wax through hydrocracking. The effect of acid property of Pd-loaded solid acid catalysts on the wax conversion and middle distillate selectivity was investigated. Co/TiO<sub>2</sub> catalyst in the first-bed reactor acted as an efficient catalyst, and produced more than 35 wt% middle distillate and more than 20 wt% wax. These heavy hydrocarbons served as a suitable feed for the production of middle distillate in the second-bed reactor. NH<sub>3</sub>-TPD experiments revealed that all the Pd-loaded solid acid catalysts retained three types of acid sites (weak-, medium-, and strong-acid sites). It was found that the wax conversion in the second-bed reactor was increased with increasing medium acidity of second-bed catalyst. Furthermore, the increment of middle distillate selectivity was roughly increased with increasing medium acidity of the catalyst. The dependencies of wax conversion and increment of middle distillate selectivity on total acidity showed the same trends as those on medium acidity. Thus, the medium acidity (total acidity) of Pd-loaded solid acid catalyst played an important role in hydrocracking of wax to middle distillate in the second-bed reactor. Among the second-bed catalysts, the Pd/MA catalyst with the highest medium acidity (total acidity) showed the best catalytic performance. The Pd/MA catalysts exhibited ca. 83% wax conversion and ca. 15 wt% increment of middle distillate selectivity, when compared to the effluent stream from the first-bed reactor.

#### Acknowledgement

The authors acknowledge the support from Korea Energy Management Corporation (2006-11-0133-3-020).

#### References

- [1] Z.-W. Liu, X. Li, K. Asami, K. Fujimoto, *Catal. Today* 104 (2005) 41–47.
- [2] A.Y. Khodakov, W. Chu, P. Fongarland, *Chem. Rev.* 107 (2007) 1692–1744.
- [3] H. Schulz, M. Claeys, *Appl. Catal. A* 186 (1999) 3–12.
- [4] H. Weyda, E. Kohler, *Catal. Today* 81 (2003) 51–55.
- [5] N. Tsubaki, Y. Yoneyama, K. Michiki, K. Fujimoto, *Catal. Commun.* 4 (2003) 108–111.
- [6] X. Dupain, R.A. Krul, C.J. Schaverien, M. Makkee, J.A. Moulijn, *Appl. Catal. B* 63 (2006) 277–295.
- [7] X. Huang, N.O. Elbashir, C.B. Roberts, *Ind. Eng. Chem. Res.* 43 (2004) 6369–6381.
- [8] A. Martínez, C. Lopez, *Appl. Catal. A* 294 (2005) 251–259.
- [9] V. Udaya, S. Rao, R.J. Gormley, *Catal. Today* 6 (1990) 207–234.
- [10] Z.-W. Liu, X. Li, K. Asami, K. Fujimoto, *Appl. Catal. A* 300 (2006) 162–169.
- [11] Z.-W. Liu, X. Li, K. Asami, K. Fujimoto, *Fuel Process. Technol.* 88 (2007) 165–170.
- [12] J. Eilers, S.A. Posthuma, S.T. Sie, *Catal. Lett.* 7 (1990) 253–270.
- [13] J.A. Brennan, P.D. Caesar, J.C. Pitman, W.E. Garwood, U.S. Patent 4,304,871 (1981).
- [14] W.O. Haag, T.J. Huang, U.S. Patent 4,159,995 (1979).
- [15] W.O. Haag, T.J. Huang, U.S. Patent 4,279,830 (1981).
- [16] S. Bessell, *Appl. Catal. A* 126 (1995) 235–244.
- [17] F.G. Botes, *Appl. Catal. A* 284 (2005) 21–29.
- [18] X. Li, K. Asami, M. Luo, K. Michiki, N. Tsubaki, K. Fujimoto, *Catal. Today* 84 (2003) 59–65.
- [19] T.-S. Zhao, J. Chang, Y. Yoneyama, N. Tsubaki, *Ind. Eng. Chem. Res.* 44 (2005) 769–775.
- [20] A. Jess, R. Popp, K. Hedden, *Appl. Catal. A* 186 (1999) 321–342.
- [21] F.G. Botes, W. Böhringer, *Appl. Catal. A* 267 (2004) 217–225.
- [22] Z.-W. Liu, X. Li, K. Asami, K. Fujimoto, *Energy Fuels* 19 (2005) 1790–1794.
- [23] Z.-W. Liu, X. Li, K. Asami, K. Fujimoto, *Catal. Commun.* 6 (2005) 503–506.
- [24] S.T. Sie, M.M.G. Senden, H.M.H. van Wechem, *Catal. Today* 8 (1991) 371–394.
- [25] Y. Rezgui, M. Guemini, *Appl. Catal. A* 282 (2005) 45–53.
- [26] K. Fang, W. Wei, F. Ren, Y. Sun, *Catal. Lett.* 93 (2004) 235–242.
- [27] S.T. Sie, *Ind. Eng. Chem. Res.* 32 (1993) 403–408.
- [28] S. Mohanty, D. Kunzru, D.N. Saraf, *Fuel* 69 (1990) 1467–1473.
- [29] D. Zhao, F. Feng, Q. Huo, N. Melosh, G.H. Fredrickson, B.F. Chmelka, G.D. Stucky, *Science* 279 (1998) 548–552.
- [30] N.N. Madikizela-Mngangeni, N.J. Coville, *J. Mol. Catal. A* 225 (2005) 137–142.
- [31] T. Oikawa, T. Ookoshi, T. Tanaka, T. Yamamoto, M. Onaka, *Micropor. Mesopor. Mater.* 74 (2004) 93–103.
- [32] J.G. Seo, M.H. Youn, K.M. Cho, S. Park, I.K. Song, *J. Power Sources* 173 (2007) 943–949.
- [33] E. Iglesia, *Appl. Catal. A* 161 (1997) 59–78.
- [34] P.J. van Berge, R.C. Everson, *Stud. Surf. Sci. Catal.* 107 (1997) 207–212.
- [35] L. Spadaro, F. Arena, M.L. Granados, M. Ojeda, J.L.G. Fierro, F. Frusteri, *J. Catal.* 234 (2005) 451–462.
- [36] Y. Zhang, M. Koike, R. Yang, S. Hinchiranan, T. Vitidsant, N. Tsubaki, *Appl. Catal. A* 292 (2005) 252–258.
- [37] H. Li, J. Li, H. Ni, D. Song, *Catal. Lett.* 110 (2006) 71–76.
- [38] H. Li, S. Wang, F. Ling, J. Li, *J. Mol. Catal. A* 244 (2005) 33–40.
- [39] D.I. Enache, M. Roy-Auberger, R. Revel, *Appl. Catal. A* 268 (2004) 51–60.
- [40] R.C. Reuel, C.H. Bartholomew, *J. Catal.* 85 (1984) 78–88.
- [41] H. Schulz, M. Claeys, *Appl. Catal. A* 186 (1999) 71–90.
- [42] A. Tavasoli, A. Khodadadi, Y. Mortazavi, K. Sadaghiani, M.G. Ahangari, *Fuel Process. Technol.* 87 (2006) 641–647.
- [43] J. Patzlauff, Y. Liu, C. Graffmann, J. Gaube, *Appl. Catal. A* 186 (1999) 109–119.
- [44] W.-P. Ma, Y.-L. Zhao, Y.-W. Li, Y.-Y. Xu, J.-L. Zhou, *React. Kinet. Catal. Lett.* 66 (1999) 217–223.
- [45] J. Gaube, H.-F. Klein, *J. Mol. Catal. A* 283 (2008) 60–68.
- [46] X. Lin, Y. Fan, Z. Liu, G. Shi, H. Liu, X. Bao, *Catal. Today* 125 (3–4) (2007) 185–191.
- [47] Y. Fan, X. Bao, G. Shi, W. Wei, J. Xu, *Appl. Catal. A* 275 (2004) 61–71.
- [48] A.R. Songip, T. Masuda, H. Kuwahara, K. Hashimoto, *Energy Fuel* 8 (1994) 131–135.
- [49] T. Masuda, H. Kuwahara, S.R. Mukai, K. Hashimoto, *Chem. Eng. Sci.* 54 (1999) 2773–2779.
- [50] A.R. Songip, T. Masuda, H. Kuwahara, K. Hashimoto, *Energy Fuel* 8 (1994) 136–140.
- [51] G. de la Puente, U.A. Sedran, *J. Catal.* 179 (1998) 36–42.
- [52] S. Jolly, J. Saussey, M.M. Bettahar, J.C. Lavalley, E. Benazzi, *Appl. Catal. A* 156 (1997) 71–96.
- [53] J.M. Arandes, M.J. Azkoiti, I. Torre, M. Olazar, P. Castaño, *Chem. Eng. J.* 132 (2007) 17–26.
- [54] A. Corma, O. Marie, F.J. Ortega, *J. Catal.* 222 (2004) 338–347.